Supporting Information

Defects Management and Efficient Photocatalytic Water Oxidation Reactions over Mg Modified $SrNbO_2N$

Xiaoqin Sun[a], Gang Liu[b] and Xiaoxiang Xu[a,*]

[a]Shanghai Key Lab of Chemical Assessment and Sustainability, School of Chemical Science and Engineering, Tongji University, 1239 Siping Road, Shanghai, 200092, China, Email: xxxu@tongji.edu.cn, telephone: +86-21-65986919

[b]Shenyang National laboratory for Materials Science, Institute of Metal Research, Chinese Academy of Science, 72 Wenhua Road, Shenyang 110016, China

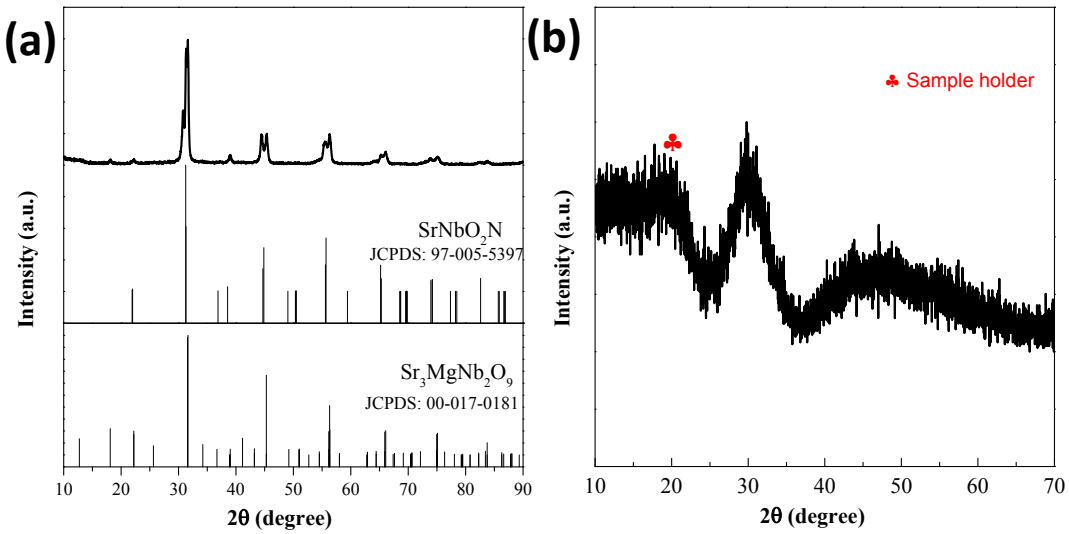

Figure S1. X-ray powder diffraction patterns of $SrMg_{0.2}Nb_{0.8}O_{2+y}N_{1-y}$ from metal oxides (a) and amorphous precursor (b).

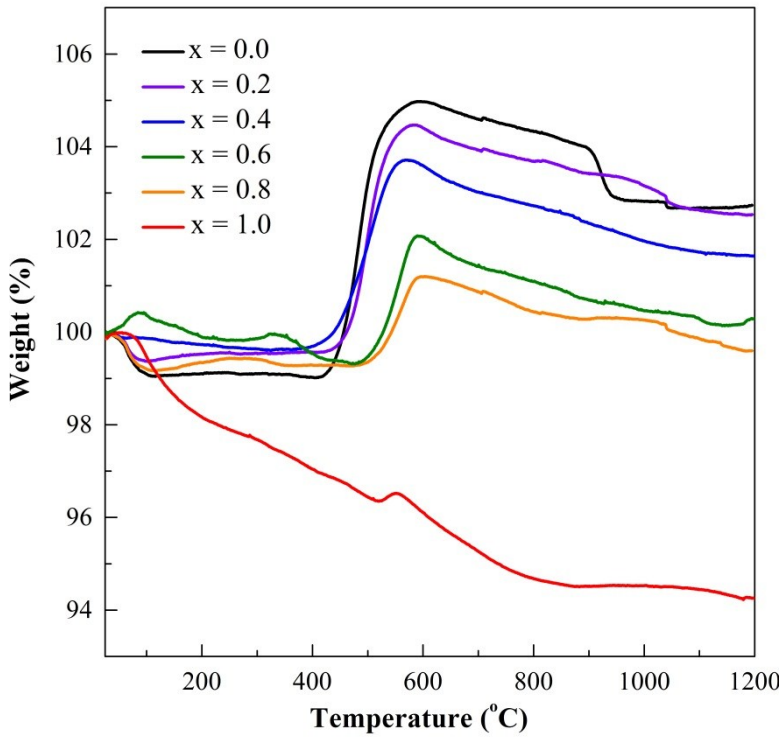

Figure S2. TGA curves of all samples in air.

Table S1. Refinements results from X-ray powder diffraction data and crystallite sizes calculated by Scherrer equation.

x	0.0	0.2	0.4	0.6	0.8	1.0
Mg/Nb U_{iso} (Å^2×100)	2.55(1)	3.11(1)	1.07(2)	1.58(2)	0.96(1)	0.62(2)
O1/N1 U_{iso} (Å^2×100)	2.18(5)	2.95(7)	4.97(3)	2.52(6)	1.35(7)	1.16(5)
O2/N2 U_{iso} (Å^2×100)	6.27(3)	6.75(2)	3.09(3)	2.08(5)	0.75(5)	0.39(2)
O1/N1 x	0	0	0	0	0	0
O1/N1 y	0	0	0	0	0	0
O1/N1 z	0.25	0.25	0.25	0.25	0.25	0.25
O2/N2 x	0.7571(3)	0.7757(5)	0.7760(4)	0.7700(4)	0.7777(7)	0.7796(6)
O2/N2 y	0.2571(1)	0.2757(1)	0.2760(2)	0.2700(4)	0.2777(5)	0.2796(2)
O2/N2 z	0	0	0	0	0	0
Nb(Mg)-O-Nb(Mg) angles (◦)	178.4(2)	174.1 (2)	178.2 (1)	175.4 (1)	173.6 (2)	173.2 (1)
Nb(Mg)-O bond distances (Å)	2.023(1)	2.022(5)	2.015(1)	2.014(3)	2.012(2)	2.010(2)
Mg SOF	0	0.06(2)	0.12(2)	0.19(2)	0.25(1)	0.32(1)
crystallite sizes (nm)	29.7(2)	22.9(1)	29.9(1)	20.5(2)	15.5(1)	15.0(1)

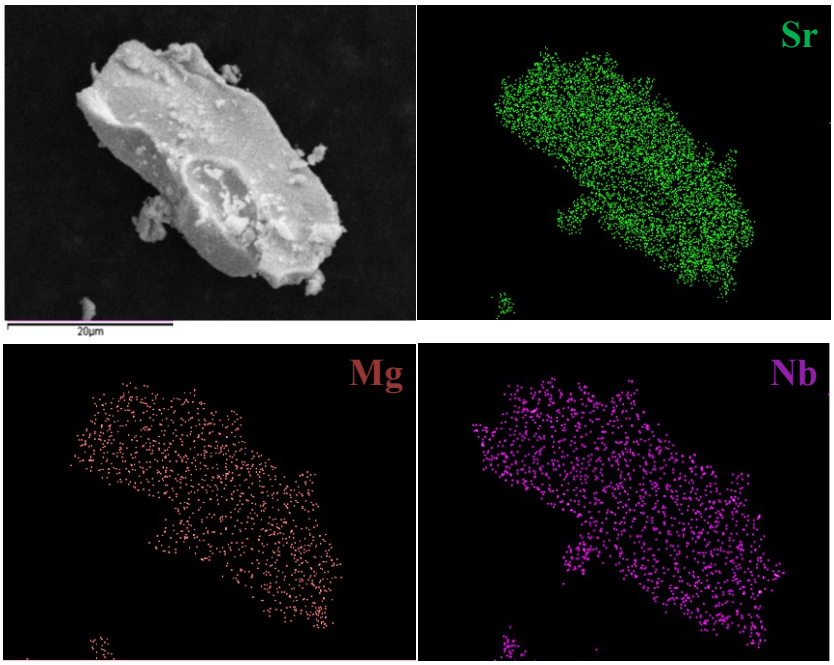

Figure S3. SEM-EDX mapping of particles of sample $SrMg_{0.2}Nb_{0.8}O_{2+y}N_{1-y}$ (x = 0.6), homogeneous Mg distribution can be identified.

Table S2 Atomic Compositions Analyzed by EDS

Sample x	**Sr/ atom%**	**Nb/ atom%**	**Mg/ atom%**	**O/ atom%**	**N/ atom%**
0	17.4	17.7	0	46.1	18.8
0.2	18.1	16.3	0.9	48.0	16.7
0.4	17.1	16.3	2.5	51.6	12.5
0.6	16.2	13.9	3.5	57.5	8.9
0.8	14.2	11.0	4.1	67.8	2.8
1	18.6	12.3	5.3	62.8	1.0

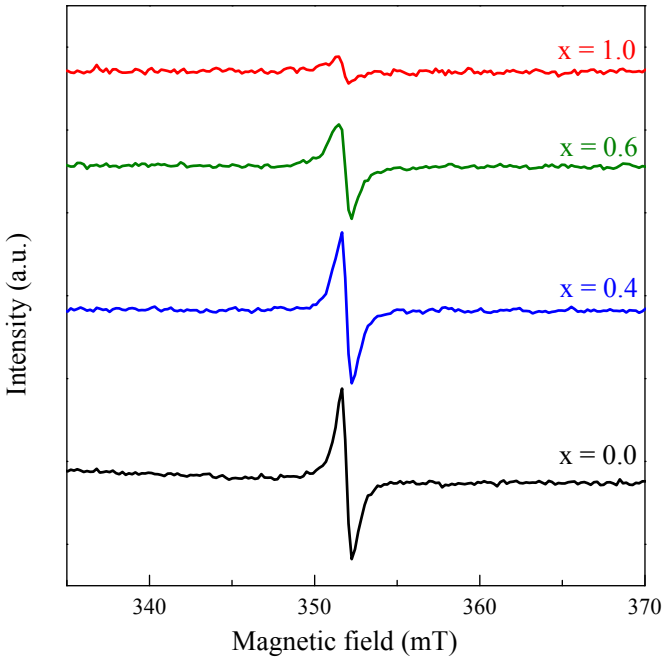

Figure S4. The electron paramagnet resonance (EPR) spectra of samples

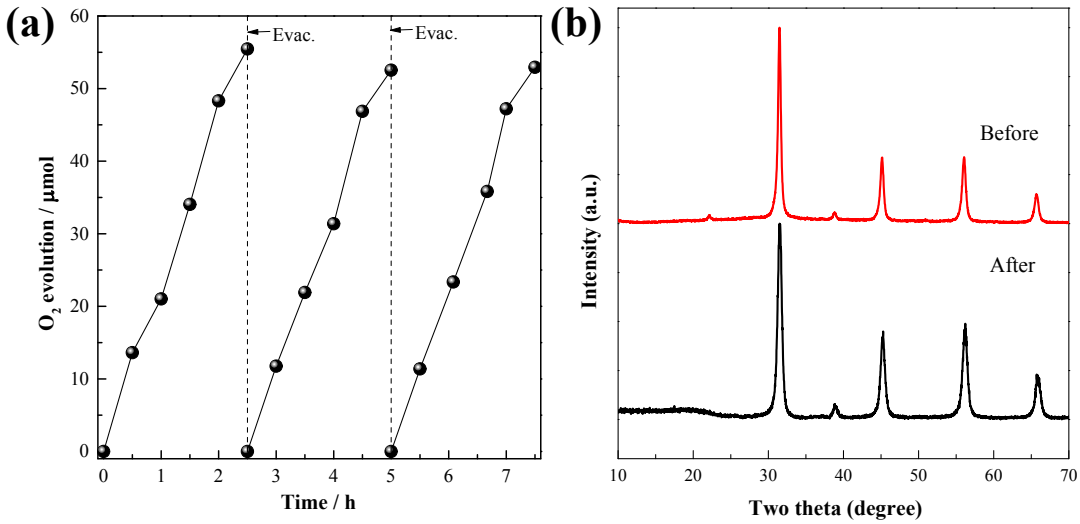

Figure S5 (a) Repeated photocatalytic oxygen evolution for $SrNb_{0.8}Mg_{0.2}O_{2+y}N_{1-y}$ under visible light illumination ($\lambda \geq 400$ nm), sodium persulfate (0.05 M) was used as a sacrificial agent. (b) XRD patterns of $SrNb_{0.8}Mg_{0.2}O_{2+y}N_{1-y}$ before and after photocatalytic experiment.

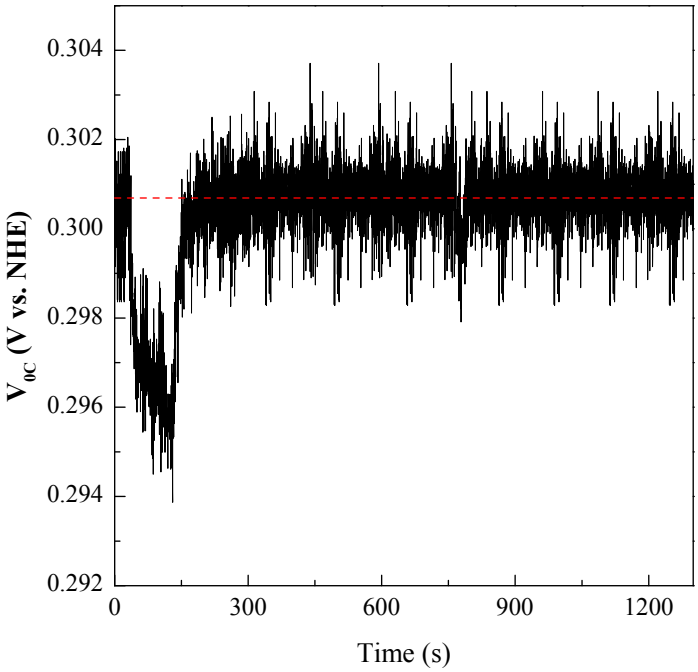

Figure S6 V_{oc} time profile of TiO_2 onto the electrodes prepared by $TiCl_4$ methanol solution

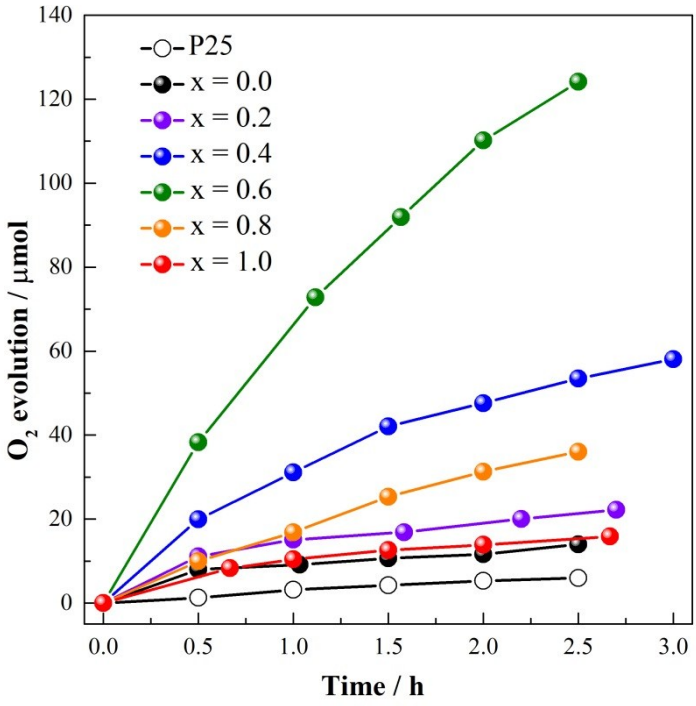

Figure S7 (a) Temporal photocatalytic oxygen evolution of as-prepared sample powders $SrMg_{x/3}Nb_{1-x/3}O_{2+y}$ N_{1-y} ($0 \leq x \leq 1$) and P25 for comparison under visible light illumination ($\lambda \geq 400$ nm), 1 wt% CoO_x was loaded as a co-catalyst and 0.05

M $AgNO_3$ aqueous solution was used as a sacrificial reagent;